V.M. PASICHNA, N.V. STOROZHUK, A.M. GUSAK

Bohdan Khmelnytsky National University of Cherkasy
(81, Shevchenko Boulevard, Cherkasy 18031, Ukraine; e-mail: pasichna.vika@ukr.net, nadushenka@ukr.net, amgusak@ukr.net)

INCUBATION TIME AT DECOMPOSITION OF SOLID SOLUTION – STOCHASTIC KINETIC MEAN-FIELD VERSUS MONTE CARLO SIMULATION

UDC 538.93

The comparison of two simulation techniques applied to the nucleation in a supersaturated solid solution is made. The first one is the well-known Monte Carlo (MC) method. The second one is a recently developed modification of the atomistic self-consistent non-linear mean-field method with the additionally introduced noise of local fluxes: Stochastic Kinetic Mean-Field (SKMF) method. The amplitude of noise is a tuning parameter of the SKMF method in its comparison with the Monte Carlo one. The results of two methods for the concentration and temperature dependences of the incubation period become close, if one extrapolates the SKMF data to a certain magnitude of the noise amplitude. The results of both methods are compared also with the Classical Nucleation Theory (CNT).

K e y w o r d s: nucleation, Monte Carlo method, solid solution, binodal, spinodal, supersaturation, noise, stochastic kinetic mean-field.

1. Introduction

The nucleation in materials physics as the first stage of first-order transformations is still a point of intense discussions concerning the choice of an evolution path, applicability of common thermodynamic parameters, competition between different sites of the heterogeneous nucleation, *etc.* The nucleation is important not only if the incubation time is large. Even if the nucleation is easy, but the system has several possible evolution paths, it always chooses the path with minimal incubation time (typically – minimal nucleation barrier). This picture is behind the well-known Ostwald rule [1–3]. Therefore, it is necessary to have a clear algorithm to calculate the incubation time for all possible evolution paths. One of these algorithms is provided by the Classical Nucleation Theory (CNT) [4–8], and another one – by the generalized Gibbs approach [9–11]. Due to experimental difficulties with measuring the nucleation parameters, much attention is paid to simulations. Most widespread are the numeric solutions of Fokker–Planck (FP) equations and Monte Carlo simulations (MC) [12]. In our paper, we will add one more technique to simulate the nucleation – Stochastic Kinetic Mean-Field method (SKMF) specially designed to include the nucleation problems [13–15]. We restrict ourselves to a rather narrow problem – homogeneous nucleation at the starting stage of the decomposition of a metastable solid solution. For this problem, we find the dependence of the mean nucleation time on the supersaturation and temperature by two simulation methods, MC and SKMF, and compare the results of these two methods and those of CNT. Namely, we check that the logarithm of the mean nucleation time approximately linearly depends on the inverse squared supersaturation (for two ways of representing the supersaturation, see below). The factor of linear dependence is

a function α of the reduced temperature $2kT/ZE_{\rm mix}$ (here, k – Boltzmann constant, $E_{\rm mix}$ – mixing energy, T – temperature, Z – number of neighbors). In Section 2, we recall the basics of CNT for the nucleation in a binary metastable solution and construct the dependence of the reduced nucleation barrier (important term in the logarithm of the incubation time) on the supersaturation (in two alternative representations) and on the reduced temperature. In Section 3, we simulate the nucleation by Monte Carlo and find the logarithm of the incubation time as a function of the supersaturation and temperature. In Section 4, we recall shortly the SKMF basic ideas and equations and then find the same parameters as in Section 3 plus the dependence on the noise amplitude. In Section 5, we compare the results of MC (Section 3), SKMF (Section 4) and CNT (Section 2): We check the hypothesis about the extrapolation of SKMF results to the maximal noise amplitude.

2. Application of Classical Nucleation Theory (CNT) to Decomposition of Metastable Regular Solid Solution

Below, we will treat the incubation time as the inverse nucleation frequency per unit volume divided by the volume of the whole system. In the steady-state approximation, this frequency (nuclei flux in the size space) is proportional to the exponent of the reduced nucleation barrier and to the Nernst–Planck diffusivity ($D_{\rm NP} = \frac{D_A D_B}{C_A D_A + C_B D_B}$) in a solid solution [7, 8]. Here, C_A, C_B- are the atomic fractions of A and B, $C_A + C_B = 1$. The classical approach within CNT for finding the nucleation barrier in the case of binary alloy is the following: Let the starting composition in a homogeneous binary solid solution be between binodal and spinodal ones. In CNT, the most favorable composition of the critical nucleus and the maximal bulk driving force per atom of a nucleus are determined by the rule of parallel tangents, shown in Fig. 1 (please, note that the rule of parallel tangents tends to the rule of common tangent, only if the supersaturation tends to zero):

$$\frac{\partial g(C_{\rm eq}+\Delta C)}{\partial \Delta C} = \frac{\partial g(C_{\rm new})}{\partial C_{\rm new}} \equiv g',$$
$$\Delta g = g(C_{\rm eq}+\Delta C) + \tag{1}$$
$$+ (C_{\rm new} - (C_{\rm eq}+\Delta C)) \cdot g' - g\,(C_{\rm new}).$$

The atomic fraction $C_{\rm new}$, defined by this rule of parallel tangents, is a composition of the emerging nucleus, corresponding to the maximum of a bulk driving force per one atom of the nucleus.

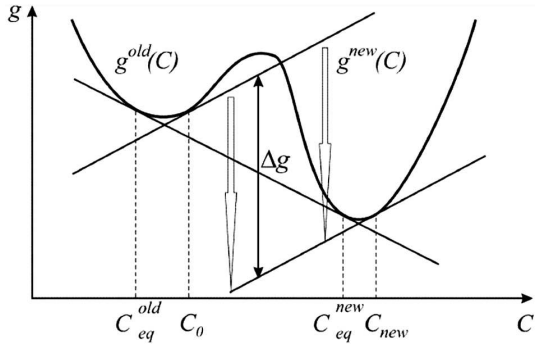

Fig. 1. Estimated driving force for the transformation of regular parallel tangents

According to CNT, this concentration corresponds to the critical nucleus. In Eq. [1], we have also the equilibrium concentration $C_{\rm eq}(T)$ (binodal point at a fixed temperature) and the initial metastable concentration $C_{\rm eq}(T) + \Delta C$ with ΔC being called the supersaturation. Another measure of a supersaturation is

$$S = \ln(C/C_{\rm eq}) = \ln\left(1 + \frac{\Delta C}{C_{\rm eq}}\right).$$

In case of small supersaturations, $\ln\left(1+\frac{\Delta C}{C_{\rm eq}}\right) \approx \approx \frac{\Delta C}{C_{\rm eq}(T)}$. In the model of regular solution, the equilibrium composition is determined by the common tangent rule in the form:

$$\frac{Z\,(1-2C_{\rm eq})}{\ln\frac{1-C_{\rm eq}}{C_{\rm eq}}} = \frac{kT}{E_{\rm mix}}. \tag{2}$$

2.1. Analytic approximation for small supersaturations

Elementary derivations using the Taylor expansion for small supersaturations lead to the following formulae:

$$\Delta g \simeq \Delta C\ (1-2C_{\rm eq})\ \frac{\partial^2 g}{\partial C^2}\bigg|_{C_{\rm eq}} = \Delta C\ (1-2C_{\rm eq}) \times$$
$$\times \left(\frac{kT}{C_{\rm eq}\,(1-C_{\rm eq})} - 2ZE_{\rm mix}\right). \tag{3}$$

Then, in case of homogeneous nucleation of the spherical nucleus, the nucleation barrier is

$$\frac{\Delta G^*}{kT} = \frac{1}{kT}\frac{1}{3}\gamma\, 4\pi \left(\frac{2\gamma\Omega}{\Delta g}\right)^2 = \alpha^{\rm theor}\,\frac{1}{(\Delta C)^2}. \tag{4}$$

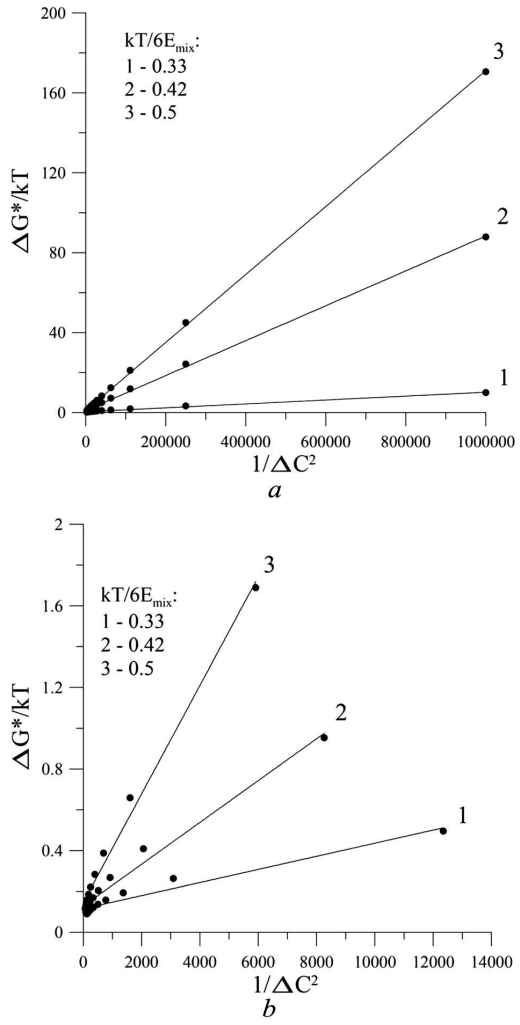

Fig. 2. Dependences of the nucleation barrier within CNT on $1/\left(\Delta C\right)^2$ at various reduced temperatures are well approximated by the linear function $\frac{\Delta G^*}{kT} \simeq \alpha^{*\mathrm{CNT}}(kT/6E_{\mathrm{mix}}) \times \times \frac{1}{(\Delta C)^2} + \beta^{*\mathrm{CNT}}$ for small supersaturations (a), but not as well at larger supersaturations (b)

Here, Ω – atomic volume, γ – surface tension between the nucleus and the mother phase, Δg can be found from Eq. (1), and the coefficient α is a following function of temperature:

$$\alpha^{\mathrm{theor}}(T) = \left(16\pi\Omega^2(\gamma/E_{\mathrm{mix}})^3 \times \right.$$
$$\left. \times \left[\frac{C_{\mathrm{eq}}\left(T\right)\left(1-C_{\mathrm{eq}}\left(T\right)\right)}{1-2C_{\mathrm{eq}}\left(T\right)}\right]^2\right)/(3(Z/2)^2 \times$$
$$\times (2kT/ZE_{\mathrm{mix}})(2kT/ZE_{\mathrm{mix}} - 4C_{\mathrm{eq}}(T)(1-C_{\mathrm{eq}}(T)))^2). \quad (5)$$

So far, we neglected the composition dependence of the surface tension. Actually, in case of solid solution, it is proportional to the squared difference of concentrations in the parent phase and in the new one. If we take the hypothesis about the validity of the parallel tangent rule in the nucleation, then this difference remains practically constant during the nucleation.

2.2. Numeric results for arbitrary supersaturations

One can also directly calculate the reduced nucleation barrier,

$$\frac{\Delta G^*}{kT} = \frac{1}{3}\gamma\, 4\pi \left(\frac{2\gamma\Omega}{\Delta g}\right)^2,$$

as a function of $1/\left(\Delta C\right)^2$.

The direct calculation demonstrates that this dependence is indeed not too far from a linear one for small supersaturations (Fig. 2, a), but substantially deviates from a linear one for larger supersaturations (Fig. 2, b):

$$\frac{\Delta G^*}{kT} \simeq \alpha^{*\mathrm{CNT}}\,\frac{1}{\left(\Delta C\right)^2} + \beta^{*\mathrm{CNT}}. \quad (6)$$

The temperature dependence of the line slopes in Fig. 2 is shown in Fig. 3

The $\ln(\tau)$ can be also expressed in terms of supersaturation parameter S (Fig. 4):

$$\frac{\Delta G^*}{kT} \simeq \alpha^{**\mathrm{CNT}}\,\frac{1}{S^2} + \beta^{**\mathrm{CNT}}. \quad (7)$$

The slopes of these dependences depend on the reduced temperature in quite another manner – compare Figs. 5 and 3. Of course, it is due to the rather sharp temperature dependence of the $\left(C_{\mathrm{eq}}\right)^2$.

One can see that, in all cases, the linear approximation of the dependence on $1/S^2$ is better. According to CNT, in the case where the nucleation is controlled by the bulk diffusion in the parent phase, the frequency of the successful nucleation per unit volume (flux of viable nuclei in the size space) is proportional to the exponent containing the sum of thermodynamic and kinetic terms:

$$j \sim \exp\left(-\frac{\Delta G^* + Q^{\mathrm{dif}}}{kT}\right). \quad (8)$$

Here, ΔG^* is a nucleation barrier, and Q^{dif} is the activation energy of interdiffusion in the parent phase:

$$\tilde{D} = \frac{D_A D_B}{C_A D_A + C_B D_B} \approx \tilde{D}_0 \exp\left(-\frac{Q^{\mathrm{dif}}}{kT}\right).$$

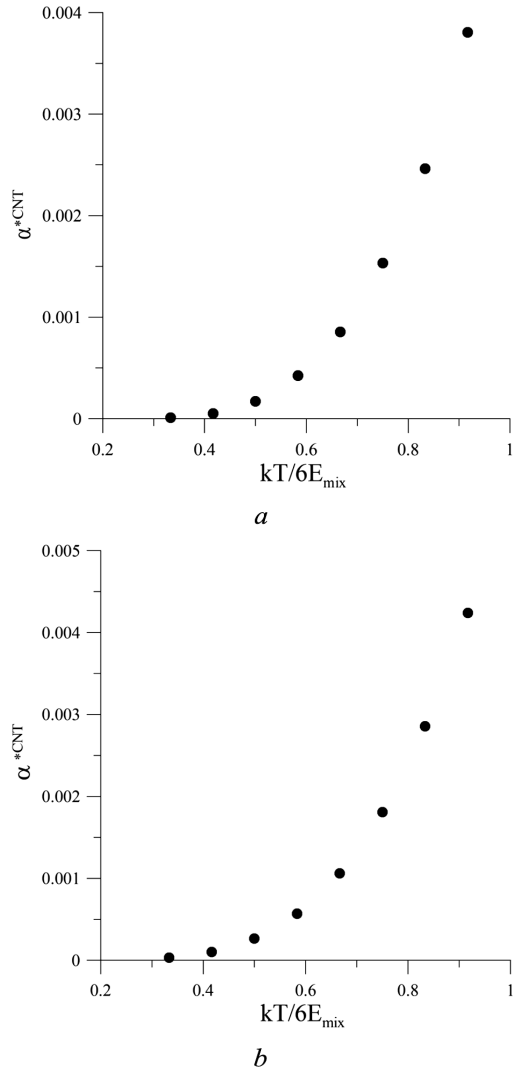

Fig. 3. Temperature dependence of the slope $\alpha^{*\mathrm{CNT}}(kT/6E_{\mathrm{mix}})$ according to CNT, for small supersaturations (a) and larger supersaturations (b)

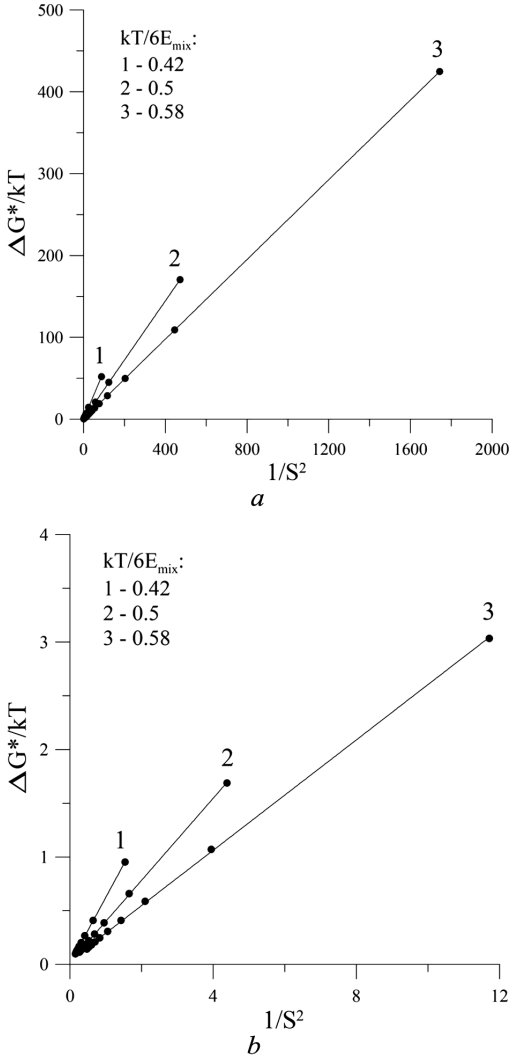

Fig. 4. Dependences of the reduced nucleation barriers on the squared inverse alternative supersaturation, for small supersaturations (a) and larger supersaturations (b), are also close to the linear functions $\frac{\Delta G^*}{kT} \simeq \alpha^{**\mathrm{CNT}}\,(kT/6E_{\mathrm{mix}})\ \frac{1}{S^2} + \beta^{**\mathrm{CNT}}$

The interesting discussion about how it is possible to combine the Arrhenius laws for the diffusivities D_A, D_B and for the interdiffusivity can be found in the classical textbook [18] and will not be discussed here. We also omit a discussion about the applicability of the Nernst–Planck (Nazarov–Gurov) expression $\tilde{D}_{\mathrm{NP}} = \frac{D_A D_B}{C_A D_A + C_B D_B}$ and the Darken expression $\tilde{D}_{\mathrm{Darken}} = C_B D_A + C_A D_B$ for different scales [3, Chapter 2] (Nernst–Planck expression is applicable on the nucleation scale). Here, it is important that ΔG^* depends strongly on the supersaturation, and Q^{dif} is almost constant within an interval of a few percent. The incubation time is inversely proportional to the nucleation frequency, so that

$$\begin{aligned} \tau &\sim \exp\left(+\frac{\Delta G^*\,(\Delta C) + Q^{\mathrm{dif}}}{kT}\right), \\ \ln\tau &\sim \frac{\Delta G^*\,(\Delta C)}{kT} + \mathrm{const}. \end{aligned} \tag{9}$$

The combination of Eqs. (6), (7), and (9) provides:

$$\ln\tau^{\mathrm{CNT}} \simeq \alpha^{*\mathrm{CNT}}\,\frac{1}{(\Delta C)^2} + \mathrm{const}, \tag{10}$$

$$\ln \tau^{\mathrm{CNT}} \simeq \alpha^{**\mathrm{CNT}} \frac{1}{\left(\ln\left(C/C_{\mathrm{eq}}\right)\right)^2} + \mathrm{const}. \qquad (11)$$

3. Monte Carlo Simulation of Nucleation

3.1. Phase diagram calculation within Monte Carlo model

The Monte Carlo model for studying the nucleation is based on the exchange mechanism of diffusion in an FCC lattice ($15 \times 15 \times 15 \times 4$ sites) with the interaction of the nearest neighbors and periodic boundary conditions. We used the Metropolis algorithm, and the "time" was counted in MC-steps. MC implicitly takes the correlation effects into account, so that the mean-field (regular solution) phase diagram is not applicable, and one should build the MC-diagram independently. To build the binodal curve, we applied the described algorithm to the diffusion couples A-B (under periodic boundary conditions) at various values of the reduced temperature $kT/6E_{\mathrm{mix}}$. The application of the diffusion couple technique to the phase diagram determination was a well-known method for decades [19, 20]. In the just cited references, this method was realized in real experiments. In virtual experiments, it was also used – by Stochastic Kinetic Mean-Field (SKMF) simulation in [21, 22] and by Monte Carlo simulation in [23]. An alternative method of phase diagram calculations is Semi-Grand Canonical Monte Carlo (SGCMC) [24]. Naturally, in the case of positive mixing energy, such simulation inevitably ends with the stepwise composition distribution – two plateau with different concentrations providing us with a binodal (solubilities as functions of the reduced mixing energy) – see Fig. 6, *a*. The resulting binodal curve is shown in Fig. 6, *b*. We compare the MC solubilities with mean-field values.

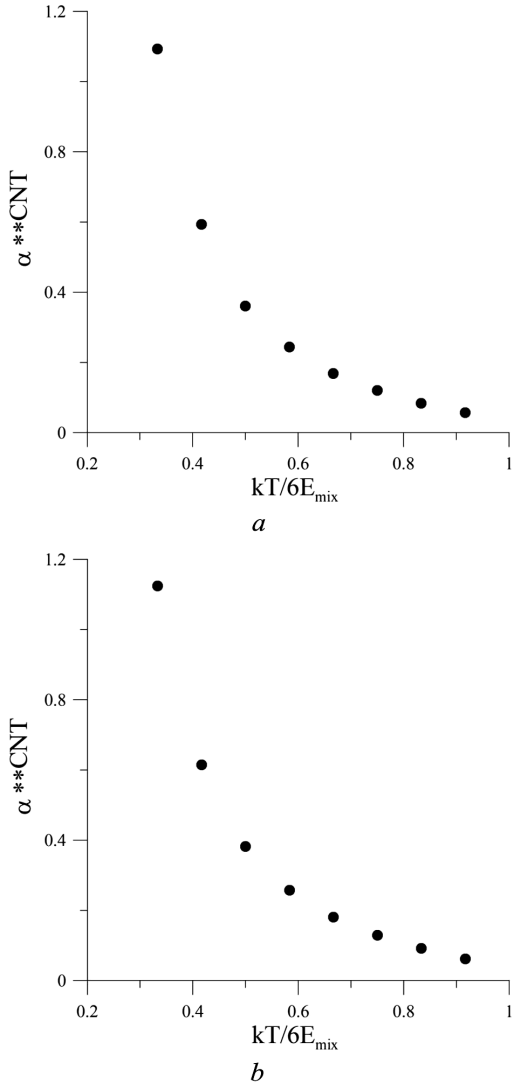

Fig. 5. Temperature dependence of the slopes $\alpha^{**\mathrm{CNT}}$ in the equation $\frac{\Delta G^*}{kT} \simeq \alpha^{**\mathrm{CNT}} \left(kT/6E_{\mathrm{mix}}\right) \frac{1}{\left(\ln\left(C/C_{\mathrm{eq}}\right)\right)^2} + \beta^{**\mathrm{CNT}}$ for small (*a*) and large (*b*) supersaturations

3.2. Criterion of nucleation in MC simulations

The atomistic simulation of a nucleation always has a problem with determining the criterion for reaching a critical nucleus size. From the point of view of thermodynamics, the critical size corresponds to the

Table 1. **Quality of the linear approximation (coefficient of determination $R^2(CNT)$) for the dependences on $1/\Delta C^2$ and $1/S^2$ at various temperatures**

$\frac{kT}{6E_{\mathrm{mix}}}$	Small supersaturation		High supersaturation	
	$1/\Delta C^2$	$1/S^2$	$1/\Delta C^2$	$1/S^2$
0.33	0.9931	1	0.9556	0.9999
0.42	0.9991	1	0.9815	0.9999
0.50	0.9998	1	0.9912	0.9999
0.58	0.9999	1	0.9956	0.9998
0.67	1	1	0.9977	0.9998
0.75	1	1	0.9985	0.9998
0.83	1	1	0.9989	0.9997
0.92	1	1	0.9992	0.9996

saddle point on the surface of the Gibbs potential as a function of the nucleus composition and size, but the random factors ("almost random walk" in a vicinity of the saddle-point state) make this picture ambiguous. CNT involves the possibility of dissolving the overcritical nucleus and the possibility of the further growth of a subcritical nucleus as a result of the random walk in the size space (Zel'dovich factor). Thus, when we were formulating the criterion, we tried to define it with "overcritical guarantee". Let us calculate, for each site of the system, the total number of atoms A in the first coordination shell and mark it as S_A. If we are interested in the formation of a nucleus around some site $(i,\ j,\ k)$, we calculate the average value of the parameter S_A in the first coordination shell of this site. The magnitude $\frac{S_A(i,\ j,\ k)}{z}$ (z – the number of nearest sites, in our case, $z = 12$) means the probability for a randomly chosen neighbor site (to this site, $(i,\ j,\ k)$) to be occupied by atom A. Let us take the sum over these probabilities on all sites of the first coordination sphere and divide it by z. The obtained parameter, as we hope, gives a value of the approximate amount of the average cluster concentration. Thus, we introduce the value $s\,(i,j,k)$:

$$s\,(i,j,k) = \frac{\sum_{q=1}^{12} S_A(i_s\,(q)\,, j_s\,(q)\,,\ k_s\,(q))}{144}, \qquad (12)$$

where i,j,k – coordinates of the site, for which the criterion of nucleation is being checked; i_s, j_s, k_s – coordinates of a neighboring site in the first coordination sphere; q – neighbor number; $S(i_s, j_s k_s)$ – the number of atoms A surrounding site (i_s, j_s, k_s) in the first coordination sphere. We take the "incubation time" as the number of Monte Carlo steps, after which the condition $s\,(i,j,k) > w$ is satisfied for this site. In this computer experiment, we choose $w = 0.95\,(1 - C_{\text{eq}})$, C_{eq} – equilibrium concentration from the Monte Carlo model. We checked that, for w larger than $0.95\,(1 - C_{\text{bin}})$, the slope of the dependence $\ln\tau \simeq \alpha\,\frac{1}{(\Delta C)^2} + \beta$ is almost insensitive to the further variation of this parameter; the slopes are shown in Fig. 7.

3.3. Results of the computer experiment

A model system in the computer experiment was characterized by two parameters – temperature and concentration of the parent phase. The incubation time was obtained as the average over the ensemble of 1000 tests with the system at same parameters. The results of the computer experiment are represented at Figs. 8–10. The obtained dependences correlate with the results of the classical nucleation theory. According to CNT, the incubation time should be inversely proportional to the flux of nuclei in the size space

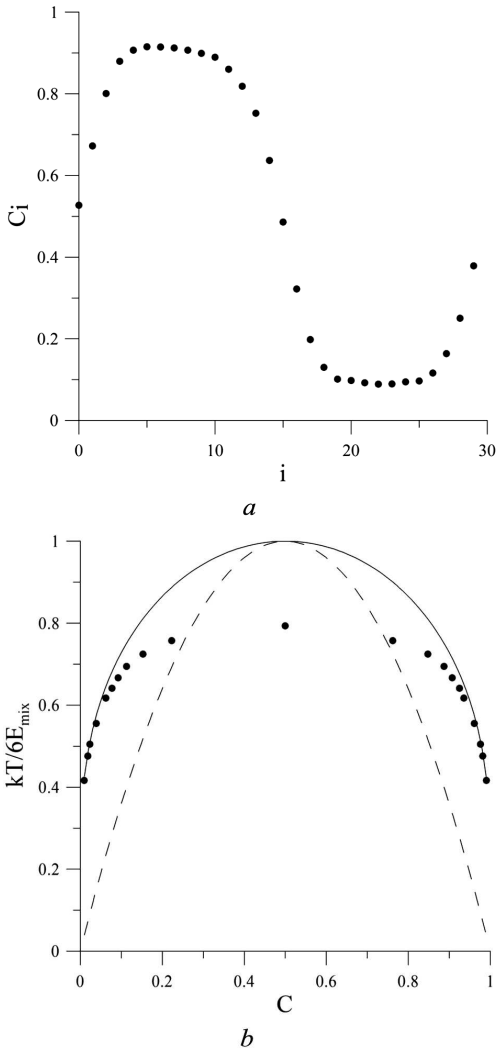

Fig. 6. Construction of the phase diagram within the MC simulation method. Typical distribution of atomic fractions (averaged upon atomic planes normal to the interdiffusion direction) along the diffusion couple with periodic boundary conditions(a), the binodal and spinodal calculated within the regular solid solution model are shown with solid and dashed lines (b), accordingly. The binodal points obtained by the Monte Carlo simulation of diffusion couples are represented with dots. As expected, the MC-cupola is lower – decomposition is harder to accomplish due to short-range order effects

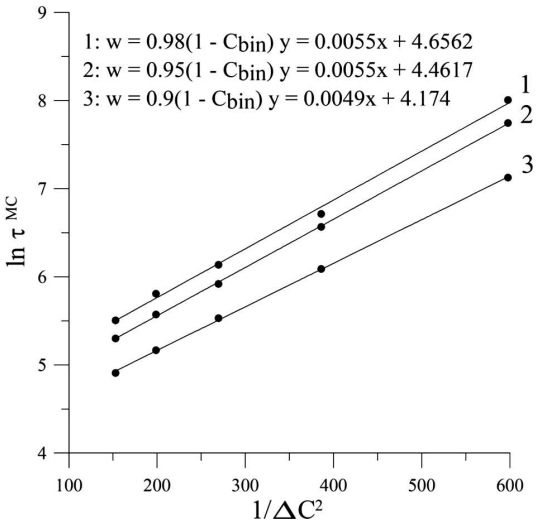

Fig. 7. Dependences of the logarithm of the incubation time on the inverse squared supersaturation at the reduced temperature $\frac{kT}{6E_{\text{mix}}} = 0.56$ at various values of the parameter w

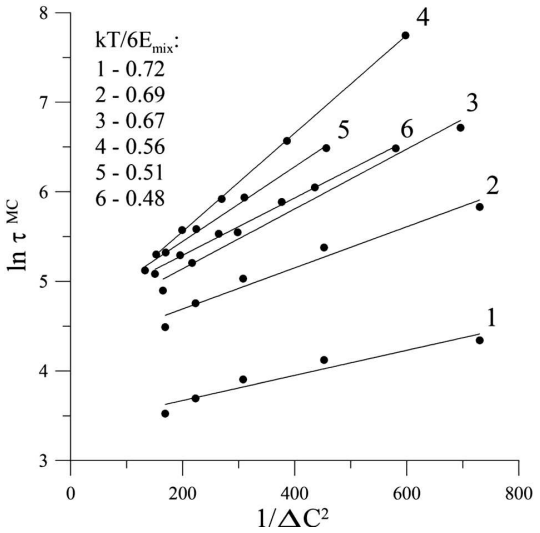

Fig. 8. Dependences of $\ln \tau^{\text{MC}}$ on $1/\left(\Delta C\right)^2$at various reduced temperatures are approximated by linear functions $\ln \tau^{\text{MC}} = \alpha^{*\text{MC}} \frac{1}{(C - C_{\text{bin}}(T))^2} + \beta^{*\text{MC}}$. Time is measured in MC steps

and, accordingly, proportional to the exponent of the height of the nucleation barrier divided by kT. As we mentioned in Section 2, CNT predicts that the logarithm of the incubation time is a linear function of the inverse squared supersaturation. Similar to Section 2, we try to approximate the logarithm of the incubation time versus the inverse squared supersaturation with two possible choices of the supersaturation parameter. The dependences in Fig. 8 can be approximated as

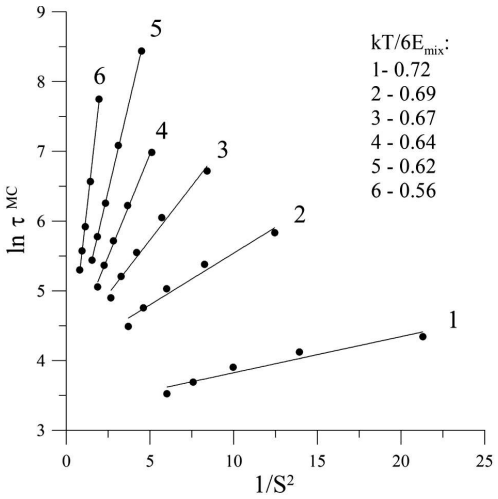

Fig. 9. Dependences of $\ln \tau^{\text{MC}}$ on $1/S^2$ at various reduced temperatures are approximated by linear functions $\frac{\Delta G^*}{kT} \simeq \simeq \alpha^{**\text{MC}} \left(kT/6E_{\text{mix}}\right) \frac{1}{\left(\ln(C/C_{\text{eq}})\right)^2} + \beta^{**\text{MC}}$. Time is measured in MC steps

$$\ln \tau^{\text{MC}} = \alpha^{*\text{MC}} \frac{1}{\left(C - C_{\text{bin}}\left(T\right)\right)^2} + \beta^{*\text{MC}}, \tag{13}$$

where $\alpha^{*\text{MC}}$ – proportionality coefficient between $\ln(\tau)$ and $\frac{1}{(C - C_{\text{bin}})^2}$; β – constant. The value of β, in theory, should be common for all dependences for the systems with fixed size. But, in this case, we have some deviation from the constant. However, these deviations are small.

Alternatively, we can approximate the logarithm of the incubation time as a linear function of the alternative supersaturation parameter $S = \ln\left(C/C_{\text{eq}}\right)$

$$\frac{\Delta G^*}{kT} \simeq \alpha^{**\text{MC}} \left(kT/6E_{\text{mix}}\right) \frac{1}{\left(\ln\left(C/C_{\text{eq}}\right)\right)^2} + \beta^{**\text{MC}}. \tag{14}$$

The results of approximations are shown in Fig. 9.

The results demonstrated in Fig. 9 are similar to those obtained in [12], but represent more values of supersaturation and temperature. Moreover, the accuracy of the linear approximation (8) is much better than that of the linear approximation (7) – see Table 2. At lower temperatures, the linear approximation is better (Table 2).

The dependences of the slopes $\alpha^{*\text{MC}}$, $\alpha^{**\text{MC}}$ in relations (13), (14) on the reduced temperature are

shown in Fig. 10. Note that Fig. 10, *b* for $\alpha^{**\mathrm{MC}}(T)$ correlates with Fig. 5 for $\alpha^{**\mathrm{CNT}}$ but Fig. 10, *a* for $\alpha^{*\mathrm{MC}}(T)$ contradicts the dependence $\alpha^{*\mathrm{CNT}}(T)$ in Fig. 3. Thus, the parameter S seems to be a more convenient measure of supersaturation.

4. Simulation of Nucleation by SKMF Method

4.1. Main equations of SKMF

The Stochastic Kinetic Mean-Field (SKMF) method or, alternatively, Stochastic Kinetic Modeling Framework, was suggested in [17, 5] and further developed in [14–16, 3, 5]. It is a non-linear self-consistent atomistic-scale version of the mean-field method with noise. It was invented as a natural development of Martin's deterministic mean-field approach. The basic kinetic equations in SKMF are the master equations formulated self-consistently for the probabilities of occupation of each site "I" by species A, with frequencies depending on the configuration energy in the mean-field approximation, and with a noise of microfluxes (or a noise of frequencies) between neighboring sites:

$$\frac{dC_i}{dt} = -\sum_{j=1}^{Z}\Big[C_i\,(1-C_j)\left(\Gamma_{i,j}^{\mathrm{mean-field}} + \delta\Gamma_{i,j}^{\mathrm{Lang}}\right) - C_j\,(1-C_i)\left(\Gamma_{j,i}^{\mathrm{mean-field}} + \delta\Gamma_{j,i}^{\mathrm{Lang}}\right)\Big], \tag{15}$$

where

$$\Gamma_{i,j}^{\mathrm{mean-field}} = \Gamma_0 \exp\left(-\frac{\overline{E_{i,j}}}{kT}\right), \tag{16}$$

$$\overline{E_{i,j}} = (M - E_{\mathrm{mix}})\sum_{l=1}^{Z=12} C_l + (M + E_{\mathrm{mix}})\sum_{n=1}^{Z=12} C_n, \tag{17}$$

$V_{\alpha,\beta}\,(\alpha,\beta = A,\ B)$ pair interaction energies with $Z = 12$ nearest neighbors, $M = (V_{AA} - V_{BB})/2$ – asymmetry parameters, $E_{\mathrm{mix}} = V_{AB} - (V_{AA} + V_{BB})/2$ – mixing energies,

$$\Gamma_0 = \nu_0 \exp\left(\frac{-E^s + Z\,(V_{AB} + V_{BB})}{kT}\right)$$

(ν_0 – frequency of attempts, E^S – saddle-point energy taken in KMF to be the same for all jumps), $\delta\Gamma_{i,j}^{\mathrm{Lang}}$ – noise of the jump frequency, $\delta\Gamma_{i,j}^{\mathrm{Lang}} = \Gamma_0 \frac{A_n}{\sqrt{\Gamma_0 dt}}\sqrt{3}\,(2\mathrm{random} - 1)$, where A_n is a

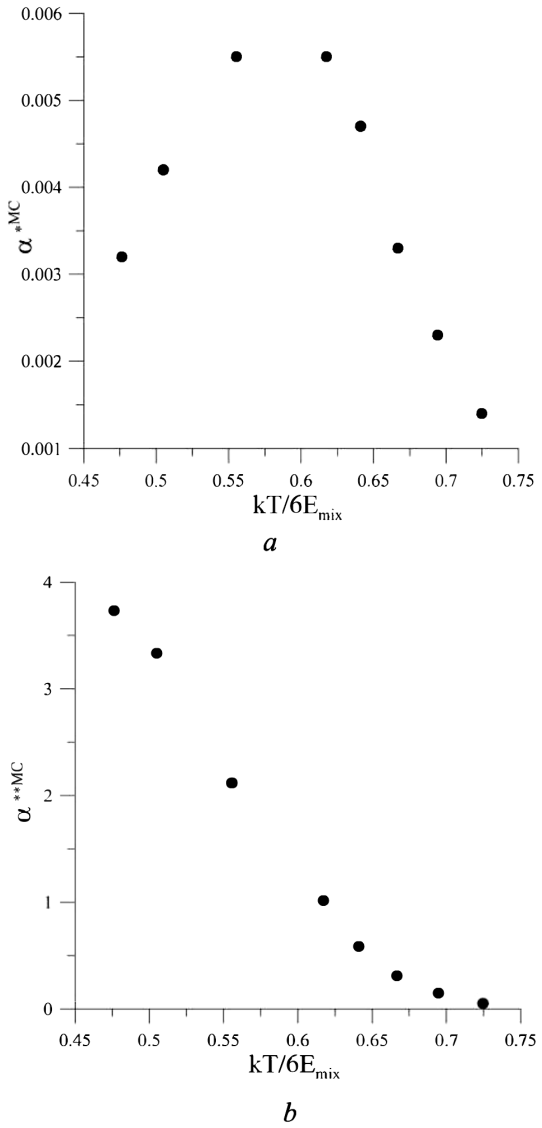

Fig. 10. Dependences of the slopes $\alpha^{*\mathrm{MC}}$ (*a*), $\alpha^{**\mathrm{MC}}$ (*b*) in relations (13), (14) on the reduced temperature $kT/6E_{\mathrm{mix}}$

Table 2. **Coefficient of determination R^2(MC) for the linear approximations (13) and (14) at various temperatures**

$kT/6E_{\mathrm{mix}}$	$1/(\Delta C)^2$	$1/S^2$
0.72	0.9245	0.9318
0.69	0.9607	0.9674
0.67	0.979	0.9847
0.64	0.9914	0.9953
0.62	0.9982	0.9997

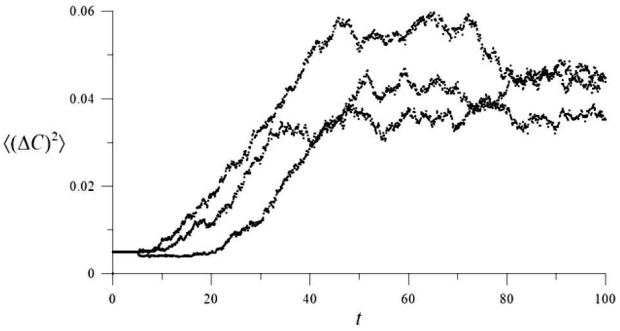

Fig. 11. Time dependence for the dispersion of the system at $\frac{kT}{6E_{\text{mix}}} = 0.42$, $C_0 = 0.10$, $A_n = 0.5$

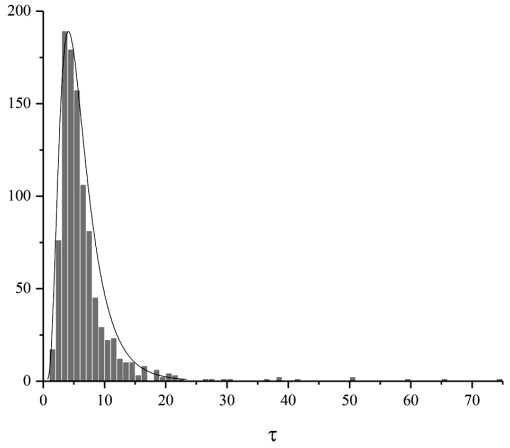

Fig. 12. Distribution of waiting times for the successful nucleation at $\frac{kT}{6E_{\text{mix}}} = 0.42$, $C_0 = 0.10$, $A_n = 0.5$. Parameters of the log-normal approximation: $\mu = 1.699424$, $\sigma = 0.533427$

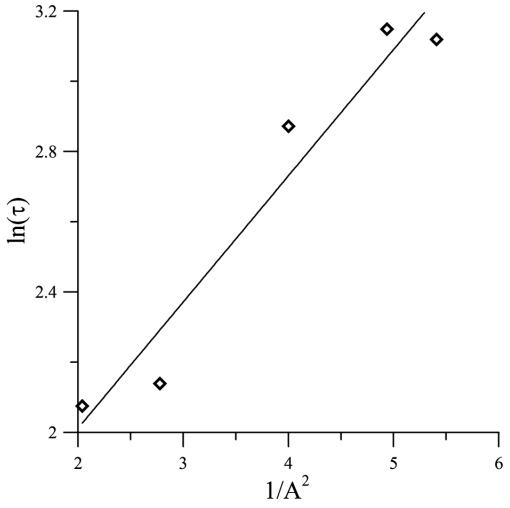

Fig. 13. Linear approximation of the $\ln\langle t_{\text{waiting}}\rangle \equiv \ln\tau$ on $\frac{1}{A^2}$

dimensionless noise amplitude, $\Gamma_0 dt$ – dimensionless time-step.

It is useful to trace the time evolution of the dispersion $\left\langle (\Delta C)^2 \right\rangle \equiv \frac{1}{N}\sum_{k=1}^{N} \left(C\left(k\right) - \langle C\rangle\right)^2$ and to check the conservation law – the temporal constancy of the mean concentration $\langle \Delta C\rangle \equiv \frac{1}{N}\sum_{k=1}^{N} C\left(k\right)$, where N is the total number of sites in the system, and $C\left(k\right)$ is the concentration at the k-th site. The typical time behavior of the dispersion is shown in Fig. 11.

The incubation time can be evaluated from the inflection point in Fig. 11. The incubation time criterion using the inflection point of the time dependence is traditional, starting from the incubation time of suppressed phases in the reactive diffusion [25]. In the Kolmogorov–Avrami kinetics for nucleation and growth [26], the time moment of the inflection point is inversely proportional to the nucleation frequence and, hence, directly proportional to the incubation time. Practically, we fixed the incubation time of decomposition, when the mean concentration in any cluster of 13 sites (central site and 12 nearest neighbors) exceeded value of 0.6.

4.2. Dependence of the incubation time on the noise amplitude

At first, we found the distribution of the waiting times. It is well approximated by the log-normal distribution – see Fig. 12.

We checked that the logarithm of the mean waiting time can be approximated (far from perfect, but still...) by a linear function of the inverse squared noise amplitude $1/A^2$:

$$\ln\tau = a\frac{1}{A^2} + b \tag{18}$$

(see Fig. 13).

4.3. Dependence of nucleation time on supersaturation of a solid solution at various temperatures

The dependences of $\ln(\tau)$ on $1/\left(\Delta C\right)^2$ at various reduced temperatures are approximated by linear functions

$$\ln(\tau) = \alpha^{*\text{SKMF}}\left(\frac{1}{\Delta C^2}\right) + \beta^{*\text{SKMF}}, \tag{19}$$

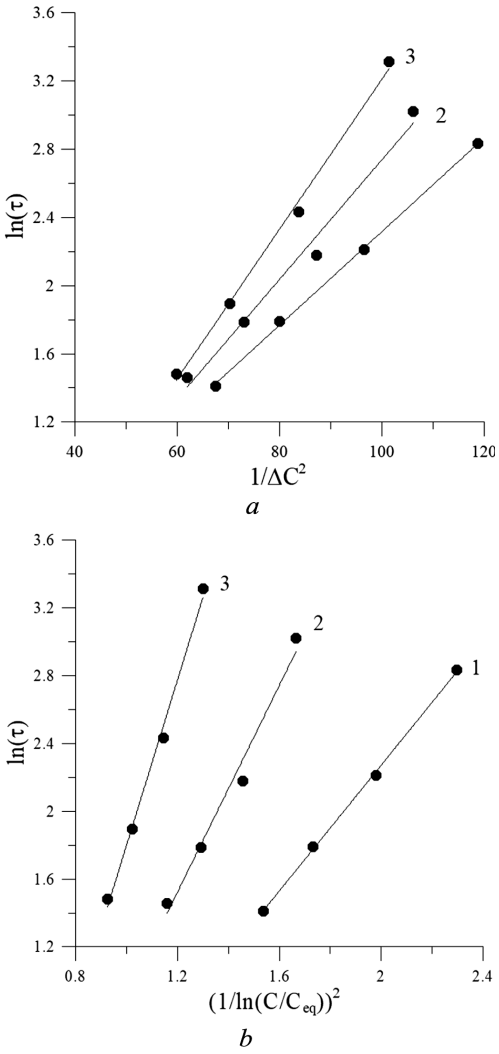

Fig. 14. Typical dependences of the logarithm of the mean incubation time on: a – $1/\left(\Delta C\right)^2$; b – $1/\left(\ln\left(\frac{C}{C_{\rm eq}}\right)\right)^2$ at the fixed noise amplitude $A = 0.6$ and (*1*) $\frac{kT}{6E_{\rm mix}} = 0.725$, (*2*) $\frac{kT}{6E_{\rm mix}} = 0.694$, (3) $\frac{kT}{6E_{\rm mix}} = 0.667$

Table 3. **Coefficient of determination R^2 (SKMF) for linear approximations in Fig. 14 at various temperatures**

$kT/6E_{\rm mix}$	$1/\left(\Delta C\right)^2$	$1/\left(\ln\left(C/C_{\rm eq}\right)\right)^2$
0.72	0.999292	0.999356
0.69	0.9856	0.98184
0.67	0.996397	0.99412
0.64	0.993599	0.99138
0.62	0.994849	0.99311

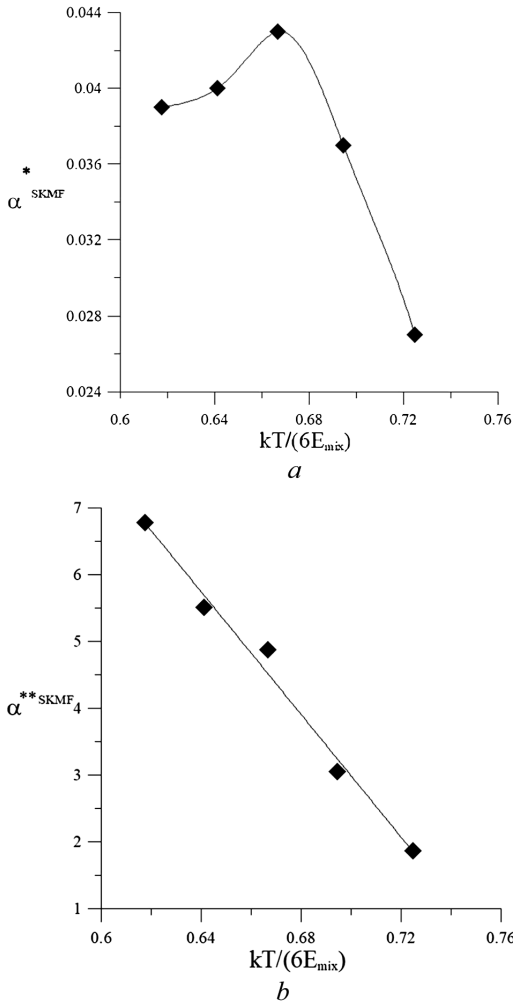

Fig. 15. Dependences of the slopes $\alpha^{*\rm SKMF}$ (a), $\alpha^{**\rm SKMF}$ (b) from Fig. 14 on the reduced temperature $kT/6E_{\rm mix}$

and the dependences of $\ln(\tau)$ on $\frac{1}{(\ln(C/C_{\rm eq}))^2}$ are approximated by linear functions

$$\ln(\tau) \simeq \alpha^{**\rm SKMF}\left(\frac{kT}{6E_{\rm mix}}\right)\frac{1}{\left(\ln\left(C/C_{\rm eq}\right)\right)^2} + \beta^{**\rm SKMF}.$$

5. Comparison of MC with Extrapolated SKMF

The simple linear dependence of the logarithm of the incubation time on the inverse squared noise amplitude allows us to check the possibility to extrapolate the results for the nucleation time to the noise amplitude, which corresponds to a single Monte Carlo sample, but cannot be simulated directly by SKMF

Table 4. **Comparison of the slopes which were obtained by CNT, MC, and SKMF extrapolated from $A = 0.6$ to $A_{\text{extrapolated}} = 1/\sqrt{\bar{C}\left(1-\bar{C}\right)}$**

$\frac{kT}{6E_{\text{mix}}}$	$\alpha^{*\text{SKMF}}\times$ $\times A^2\bar{C}\left(1-\bar{C}\right)$	$\alpha^{*\text{MC}}$	$\alpha^{*\text{CNT}}$ for large ΔC	$\alpha^{**\text{SKMF}}\times$ $\times A^2\bar{C}\left(1-\bar{C}\right)$	$\alpha^{**\text{MC}}$	$\alpha^{**\text{CNT}}$ for big S
0.725	0.00158	0.0014	0.0016	0.11	0.05	0.14
0.694	0.00209	0.0023	0.0013	0.17	0.15	0.16
0.667	0.00233	0.0033	0.0011	0.27	0.31	0.18
0.641	0.00208	0.0047	0.0009	0.29	0.59	0.20
0.617	0.00193	0.0055	0.0007	0.34	1.01	0.22

due to the divergence problems. As shown in [13] for the ideal solution and in [15] for a regular solution, the finite noise amplitude corresponds to the averaging over a finite number of MC runs (or, equivalently, over the finite number M of copies of the canonical ensemble). Namely,

$$M = \frac{1}{\bar{C}\left(1-\bar{C}\right)A^2}. \tag{20}$$

Monte Carlo simulations of the nucleation correspond to the case $M = 1$, which means that the SKMF should be close to MC, if we extrapolate the results obtained at some noise amplitude A to the extrapolated value

$$A^2_{\text{extrapolated}} = \frac{1}{\bar{C}\left(1-\bar{C}\right)}. \tag{21}$$

Based on the linear dependence (14) of $\ln\tau$ on the inverse squared noise amplitude, one may suggest the following approximate correspondence:

$$\frac{A^2}{A^2_{\text{extrapolated}}}\left.\frac{\Delta\ln\tau}{\Delta\left(\frac{1}{\Delta C^2}\right)}\right|_A = A^2\bar{C}\left(1-\bar{C}\right)\left.\frac{\Delta\ln\tau}{\Delta\left(\frac{1}{\Delta C^2}\right)}\right|_A \approx$$

$$\approx \left.\frac{\Delta\ln\tau}{\Delta\left(\frac{1}{\Delta C^2}\right)}\right|_{\text{MC}} \text{and/or} \left.\frac{\Delta\ln\tau}{\Delta\left(\frac{1}{\Delta C^2}\right)}\right|_{\text{CNT}}, \tag{22}$$

$$A^2\bar{C}\left(1-\bar{C}\right)\left.\frac{\Delta\ln\tau}{\Delta\left(\ln\left(C/C_{\text{eq}}\right)\right)^2}\right|_A \approx$$

$$\approx \left.\frac{\Delta\ln\tau}{\Delta\left(\ln\left(C/C_{\text{eq}}\right)\right)^2}\right|_{\text{MC}} \text{and/or} \left.\frac{\Delta\ln\tau}{\Delta\left(\ln\left(C/C_{\text{eq}}\right)\right)^2}\right|_{\text{CNT}}. \tag{23}$$

One can see from Table 4 that the slopes obtained from extrapolated SKMF are situated almost always between the values obtained from Classical Nucleation Theory and Monte Carlo. In the only case (for α^{**} at $\frac{kT}{6E_{\text{mix}}} = 0.694$), when the extrapolated SKMF value is a little bit beyond the interval (MC-CNT), they are practically the same: $0.17 \approx 0.16 \approx 0.15$.

6. Conclusions

1. Computer simulations using the Monte Carlo and Stochastic Kinetic Mean-Field methods predict the approximate linear dependence of the logarithm of the incubation time on the inverse squared supersaturation at the decomposition of a solid solution – Eqs. (13), (19). It corresponds to the semianalytic prediction of CNT [Eq. (10)].

2. The linear approximation reached for the dependence on the inverse squared $S \equiv \ln\left(C/C_{\text{eq}}\right)$ is better than for the inverse squared $(C - C_{\text{eq}})$ – Eqs. (14), (20), (11).

3. Results of SKMF modeling depend, naturally, on the noise amplitude A: the logarithm of the incubation time linearly increases with the inverse squared noise amplitude [Eq. (18)].

4. To predict the realistic incubation time, one should extrapolate the results of SKMF simulations according to Eqs. (23), (24).

5. After the extrapolation, the results of SKMF appear to be intermediate between Monte Carlo and CNT (Table 3). The interpretation of the temperature dependence of the slope α will be proposed elsewhere.

This work was supported by Ministry of Education and Science of Ukraine (project 0118U003861).

1. W. Ostwald. Zeitschrift fur physikalische. *Chemie* **22** (1), 289 (1897).

2. J.W.P. Schmelzer, A.S. Abyzov. *How do Crystals Nucleate and Grow: Ostwald's Rule of Stages and Beyond* (Springer, 2017) [ISBN: 978-3-319-45899-1].
3. A.M. Gusak, T.V. Zaporozhets, Y.O. Lyashenko, S.V. Kornienko, M.O. Pasichnyy, A.S. Shirinyan. Diffusion-controlled solid state reactions. In: *Alloys, Thin Films, and Nanosystems* (Wiley, 2010) [ISBN: 978-3-527-40884-9].
4. D. Turnbull, J.C. Fisher. Rate of nucleation in condensed systems. *J. Chem. Phys.* **17** (1), 71 (1949).
5. K. Kelton, A.L. Greer. *Nucleation in Condensed Matter: Applications in Materials and Biology* (Elsevier, 2010) [ISBN: 978-0-08-042147-6].
6. O.Y. Liashenko, A. Gusak, F. Hodaj. Spectrum of heterogeneous nucleation modes in crystallization of Sn-0.7 wt Cu solder: Experimental results versus theoretical model calculations. *J. Mater. Sci.: Mater. Electron.* **26** (11), 8464 (2015).
7. *Nucleation Theory and Applications*, edited by J.W.P. Schmelzer (Wiley, 2006) [ISBN-13: 978-3-527-40469-8, ISBN-10:3-527-40469-8].
8. V.V. Slezov. *Kinetics of First-Order Phase Transitions* (Wiley, 2009) [ISBN: 978-3-527-40775-0].
9. A.S. Abyzov, J.W. Schmelzer. Kinetics of segregation processes in solutions: Saddle point versus ridge crossing of the thermodynamic potential barrier. *J. Non-Crystalline Solids* **384**, 8 (2014).
10. J.W. Schmelzer, A.S. Abyzov, J. Moller. Nucleation versus spinodal decomposition in phase formation processes in multicomponent solutions. *J. Chem. Phys.* **121** (14), 6900 (2004).
11. A.S. Abyzov, J.W. Schmelzer, L.N. Davydov. Heterogeneous nucleation on rough surfaces: Generalized Gibbs' approach. *J. Chem. Phys.* **147** (21), 214705 (2017).
12. F. Soisson, G. Martin. Monte Carlo simulations of the decomposition of metastable solid solutions: Transient and steady-state nucleation kinetics. *Phys. Rev. B* **62** (1), 203 (2000).
13. Z. Erdelyi, M. Pasichnyy, V. Bezpalchuk, J.J. Toman, B. Gajdics, A.M. Gusak. Stochastic kinetic mean field model. *Comp. Phys. Commun.* **204**, 31 (2016).
14. V. Bezpalchuk, R. Kozubski, M. Pasichnyy, A. Gusak. Tracer diffusion and ordering in FCC structures-stochastic kinetic Mean-Field Method vs. Kinetic Monte Carlo. *Defect and Diffusion Forum* **383**, 59 (2018).
15. A. Gusak, T. Zaporozhets. Martin's kinetic mean-field model revisited–frequency noise approach versus Monte Carlo. *Metallofiz. Noveish. Tekhnol.* **40** (11), 1415 (2018).
16. B. Gajdics, J.J. Toman, H. Zapolsky, Z. Erdelyi, G. Demange. A multiscale procedure based on the stochastic kinetic mean field and the phase-field models for coarsening. *J. Appl. Phys.* **126** (6), 065106 (2019).
17. N.V. Storozhuk, K.V. Sopiga, A.M. Gusak. Mean-field and quasi-phase-field models of nucleation and phase competition in reactive diffusion. *Philosophical Magazine* **93** (16), 1999 (2013).
18. A.A. Smirnov. *Molecular Kinetic Theory of Metals* (Nauka, 1966) (in Russian) [ISBN: 978-5-02].
19. A.A. Kodentsov, G.F. Bastin, F.J.J. Van Loo. The diffusion couple technique in phase diagram determination. *J. Alloys and Compounds* **320** (2), 207 (2001).
20. J.C. Zhao. Reliability of the diffusion-multiple approach for phase diagram mapping. *J. Mater. Sci.* **39** (12), 3913 (2004).
21. Z. Erdelyi, M. Pasichnyy, V. Bezpalchuk, J.J. Toman, B. Gajdics, A.M. Gusak. Stochastic kinetic mean field model. *Comp. Phys. Commun.* **204**, 31 (2016).
22. A. Gusak, T. Zaporozhets, N. Storozhuk. Phase competition in solid-state reactive diffusion revisited-stochastic kinetic mean-field approach. *J. Chem. Phys.* **150** (17), 174109 (2019).
23. C. Hin, J. Lepinoux, J.B. Neaton, M. Dresselhaus. From the interface energy to the solubility limit of aluminium in nickel from first-principles and kinetic Monte Carlo calculations. *Mater. Sci. Engin.: B* **176** (9), 767 (2011).
24. A. Biborski, L. Zosiak, R. Kozubski, R. Sot, V. Pierron-Bohnes. Semi-grand canonical Monte Carlo simulation of ternary bcc lattice-gas decomposition: Vacancy formation correlated with B2 atomic ordering in A–B intermetallics. *Intermetallics* **18** (12), 2343 (2010).
25. M. Pasichnyy, A. Gusak. Modeling of phase competition and diffusion zone morphology evolution at initial stages of reaction diffusion *Defect and Diffusion Forum* **237**, 1193 (2005).
26. C. Michaelsen, K. Barmak, T.P. Weihs. Investigating the thermodynamics and kinetics of thin film reactions by differential scanning calorimetry. *J. Phys. D: Appl. Phys.* **30** (23), 3167 (1997).

Received 30.09.19

В.М. Пасічна, Н.В. Сторожук, А.М. Гусак

ІНКУБАЦІЙНИЙ ЧАС РОЗПАДУ ТВЕРДОГО РОЗЧИНУ – СТОХАСТИЧНИЙ КІНЕТИЧНИЙ МЕТОД СЕРЕДНЬОГО ПОЛЯ У ПОРІВНЯННІ З МЕТОДОМ МОНТЕ-КАРЛО

Р е з ю м е

Зроблено порівняння двох методів, які застосовуються для моделювання зародкоутворення в пересиченому твердому розчині. Перший – це добре відомий метод Монте-Карло (МК). Другий – нещодавно розроблена модифікація атомістичного самоузгодженого нелінійного методу середнього поля з додатково введеним шумом локальних потоків – стохастичний кінетичний метод середнього поля (SKMF). Амплітуда шуму є параметром налаштування методу SKMF у порівнянні його з методом МК. Результати двох методів для концентраційної та температурної залежності інкубаційного періоду стають близькими, якщо екстраполювати дані SKMF до певної величини амплітуди шуму. Результати обох методів порівнюються також з класичною теорією зародкоутворення (CNT).